Rotationally resolved electronic spectra of 9,10-dihydrophenanthrene. A "floppy" molecule in the gas phase

Leonardo Alvarez-Valtierra and David W. Pratt[a)]
Department of Chemistry, University of Pittsburgh, Pittsburgh, Pennsylvania 15260

(Received 2 March 2007; accepted 28 March 2007; published online 13 June 2007)

Rotationally resolved fluorescence excitation spectra of several bands in the $S_1 \leftarrow S_0$ electronic spectrum of 9,10-dihydrophenanthrene (DHPH) have been observed and assigned. Each band was fit using rigid rotor Hamiltonians in both electronic states. Analyses of these data reveal that DHPH has a nonplanar configuration in its S_0 state with a dihedral angle between the aromatic rings (φ) of $\sim 21.5°$. The data also show that excitation of DHPH with UV light results in a more planar structure of the molecule in the electronically excited state, with $\varphi \sim 8.5°$. Three prominent Franck-Condon progressions appear in the low resolution spectrum, all with fundamental frequencies lying below 300 cm^{-1}. Estimates of the potential energy surfaces along each of these coordinates have been obtained from analyses of the high resolution spectra. The remaining barrier to planarity in the S_1 state is estimated to be ~ 2650 cm^{-1} along the bridge deformation mode and is substantially reduced by excitation of the molecule along the (orthogonal) ring twisting coordinate. © *2007 American Institute of Physics*.
[DOI: 10.1063/1.2732753]

I. INTRODUCTION

Low frequency vibrational modes in large molecules have been extensively studied in the past years owing to their relevance in a wide variety of processes in chemical physics. These processes include intramolecular vibrational redistribution, the Duschinsky effect, Herzberg-Teller couplings, internal conversion, intersystem crossing, and many others.[1–7] Low frequency modes are relevant in these processes because they create a high density of states at the available energy, making possible rapid energy redistribution among these modes even when there are only small couplings among them.[8]

Typical low frequency modes in large molecules possessing different functional groups include inversions, torsions, ring twists, butterfly motions, and other large amplitude out-of-plane vibrations.[9–15] An interesting example is provided by 9,10-dihydrophenanthrene (DHPH), see Scheme 1 below. DHPH is a homolog of stilbene and has figured

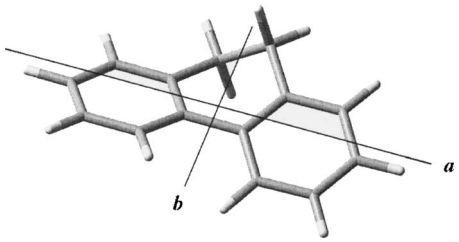

SCHEME 1. Optimized structure of DHPH in its S_0 state.

prominently in discussions of *cis-trans* photoisomerization dynamics.[16] Previously, Chakraborty and Chowdhury (CC),[17] Zgierski *et al.* (ZZSL),[18] and Smith and Knee[19] (SK) have performed a number of low resolution fluorescence excitation, emission, and depletion experiments on DHPH cooled in a supersonic jet. All authors observed essentially identical excitation spectra. The molecule exhibits an extensive, strong, and apparently harmonic progression with a fundamental frequency of ~ 100 cm^{-1}, and apparently similar progressions of somewhat lower intensity at higher energies. However, the aforementioned authors differ in their interpretations of these modes. CC assigned the main progression to an out-of-plane torsional mode, ZZSL assigned it to an out-of-plane nontotally symmetric $-CH_2-CH_2-$ bridge deformation mode, and SK assigned it to a totally symmetric phenyl torsional mode that is governed by a single-minimum potential rather than a double-minimum one.

Described herein is an extensive study of the rotationally resolved $S_1 \leftarrow S_0$ fluorescence excitation spectra of several of the bands exhibited in the low resolution spectrum of DHPH. The data show that the molecule is nonplanar in its S_0 state with a dihedral angle between the rings of $\varphi \sim 21.5°$; that the molecule is also nonplanar in its S_1 state, but with a smaller dihedral angle ($\varphi \sim 8.5°$); and that three vibrational modes are active in flattening the molecule when it is excited to the S_1 state. Each of these modes have been identified; mode *a* is a ring twisting mode, mode *b* is a combined in-plane-bending and stretching mode, and mode *c* is a bridge deformation mode. Potential energy surfaces along each of these coordinates have been determined from analyses of these spectra. Additionally, the data show that there is a strong coupling of all these modes in the S_1 state, and that excitation of the ring twisting mode substantially reduces the barrier to planarity along the bridge deformation mode.

[a)]Author to whom correspondence should be addressed. Electronic mail: pratt@pitt.edu

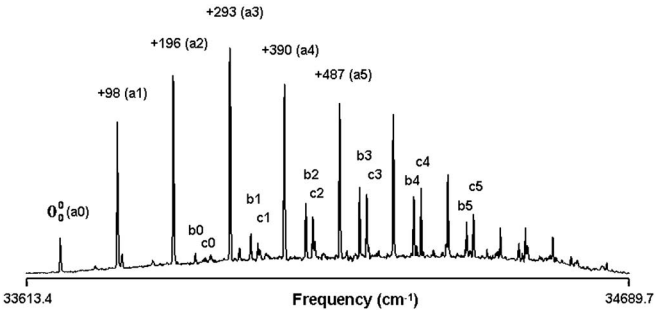

FIG. 1. Vibrationally resolved fluorescence excitation spectrum of DHPH in the gas phase.

II. EXPERIMENT

DHPH (>94% pure) was purchased from Aldrich and used without further purification. Dry argon (Ar) was used in all experiments as an inert carrier gas.

In the vibrationally resolved fluorescence excitation experiments, samples were seeded into 20 psi of Ar gas and expanded into a vacuum chamber (10^{-5} torr) through a 1 mm diameter orifice pulsed valve (General Valve Series 9) operating at 10 Hz. Two cm downstream of the valve, the free jet was excited with the second harmonic of a Quanta Ray Nd^{3+}: YAG (Model DCR-1A) pumped dye laser (Model PDL-1). The dye (Kiton Red 620) laser output was frequency doubled with an external KDP crystal providing a spectral resolution of ~0.6 cm^{-1} in the ultraviolet (UV). The molecules were excited at the point of intersection between the jet and the laser beam and the resulting fluorescence was collected with a photomultiplier tube (PMT). Finally, the collected data were processed by a boxcar integrator (Stanford Research Systems) and recorded with QUICK DATA ACQUISITION software (Version 1.0.5).

Rotationally resolved experiments were performed using a molecular beam laser spectrometer, described in detail elsewhere.[20] Briefly, the molecular beam was formed by expansion of vaporized DHPH seeded in Ar (−15 psi) through a heated (~425 K) 200 μm quartz nozzle into a differentially pumped vacuum system. The expansion was skimmed 2 cm downstream with a 1 mm diameter skimmer and crossed 13 cm further downstream by a continuous wave (cw) Ar^+-pumped ring dye laser. The cw laser was operated with Rhodamine 6G dye and intracavity frequency doubled in a BBO crystal, yielding ~200 μW of UV radiation with a resolution of ~1 MHz. The fluorescence excitation spectrum was detected, using spatially selective optics, by a PMT and photon counting system. The PMT signal together with the iodine absorption spectrum and the relative frequency markers were simultaneously collected and processed by the JB95A data acquisition system.[20] Absolute frequency calibration of the spectra was performed by comparison with the I_2 absorption spectrum. Relative frequency markers were obtained from a stabilized etalon having a free spectral range of 299.7520±0.0005 MHz.

III. RESULTS

Figure 1 shows the vibrationally resolved fluorescence excitation (low resolution) spectrum of DHPH. In agreement with previous results,[18,19] we observe three well-defined Franck-Condon (FC) progressions of vibrational bands, labeled **a**, **b**, and **c** in Fig. 1. Clearly, these long FC progressions signal large differences in the potential energy surfaces along different low frequency coordinates of the molecule in both electronic states. The first (**a**) progression is the most intense one, while the second and the third progressions are weaker, blueshifted in frequency, and have similar intensities. The labeling scheme used in Fig. 1 is analogous to the one used by ZZSL.[18] The 0_0^0 transition is located at 33 669.9 cm^{-1} (~297 nm), blueshifted from that of phenanthrene by more than 43 nm,[21] and redshifted from that of

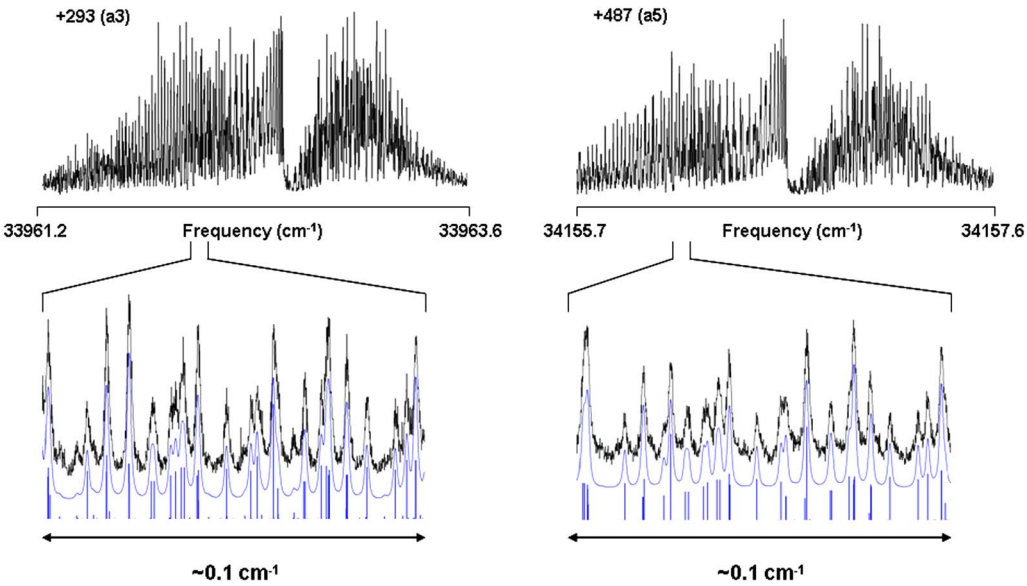

FIG. 2. Rotationally resolved fluorescence excitation spectra of the bands at +293 cm^{-1} (**a3**) and +487 cm^{-1} (**a5**) in the first Franck-Condon progression of DHPH in the gas phase (top panels). Equivalent portions of the *P* branches at full experimental resolution and the corresponding simulated spectra with and without an assumed line shape function are also shown (bottom panels).

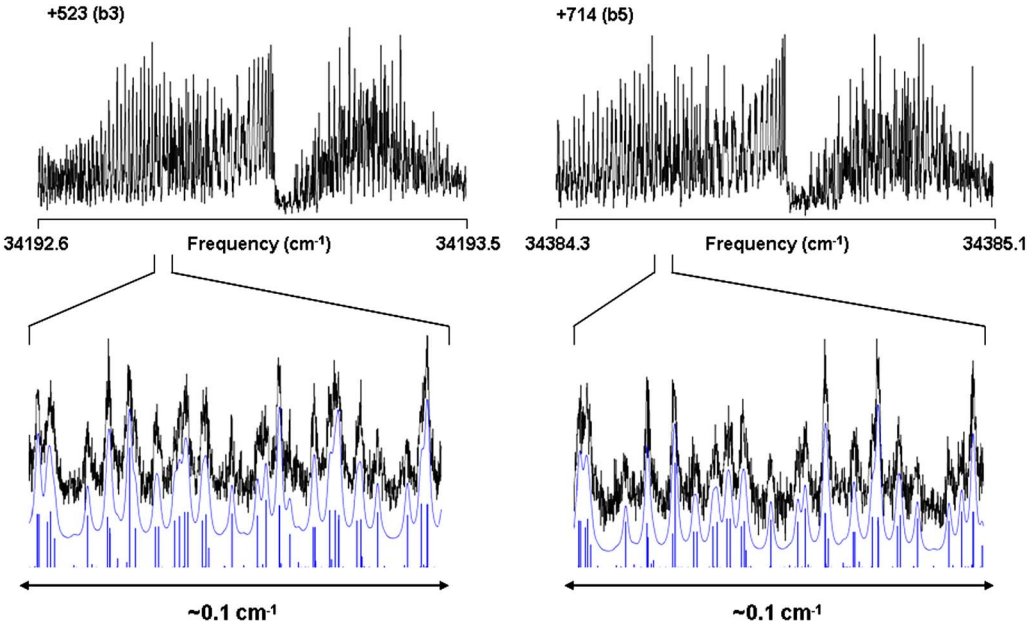

FIG. 3. Rotationally resolved fluorescence excitation spectra of the bands at +523 (**b3**) and +714 cm^{-1} (**b5**) in the second Franck-Condon progression of DHPH in the gas phase (top panels). Equivalent portions of the *P* branches at full experimental resolution and the corresponding simulated spectra with and without an assumed line shape function are also shown (bottom panels).

biphenyl by ~13.5 nm.[22] The frequency spacing among the members of the **a** progression has a nearly constant value of ~97.5 cm^{-1}. The **b** and **c** FC progressions exhibit similar spacings but their "false" origins are shifted to the blue of the "true" origin by ~234 and ~246 cm^{-1}, respectively.

Extensive studies of several of these bands have been performed at high resolution. Our first examples are from the **a** progression. Figure 2 shows the rotationally resolved $S_1 \leftarrow S_0$ fluorescence excitation spectra of the bands at +293 cm^{-1} (**a3**) and +487 cm^{-1} (**a5**). Each spectrum spans ~2 cm^{-1} and exhibits pure *a*-type character. To fit these spectra, we first generated about 4500 *a*-type rovibronic transitions based on *ab initio*[23] estimates of rotational constants and rigid rotor Hamiltonians for both electronic states. Then, we made quantum number assignments of single transitions in each of the simulated spectra to the corresponding transitions in each of the experimental spectra, using the Windows-based program JB95.[24] Finally, we used a least-squares fitting procedure to optimize the rotational constants, based on a comparison of observed and calculated line posi-

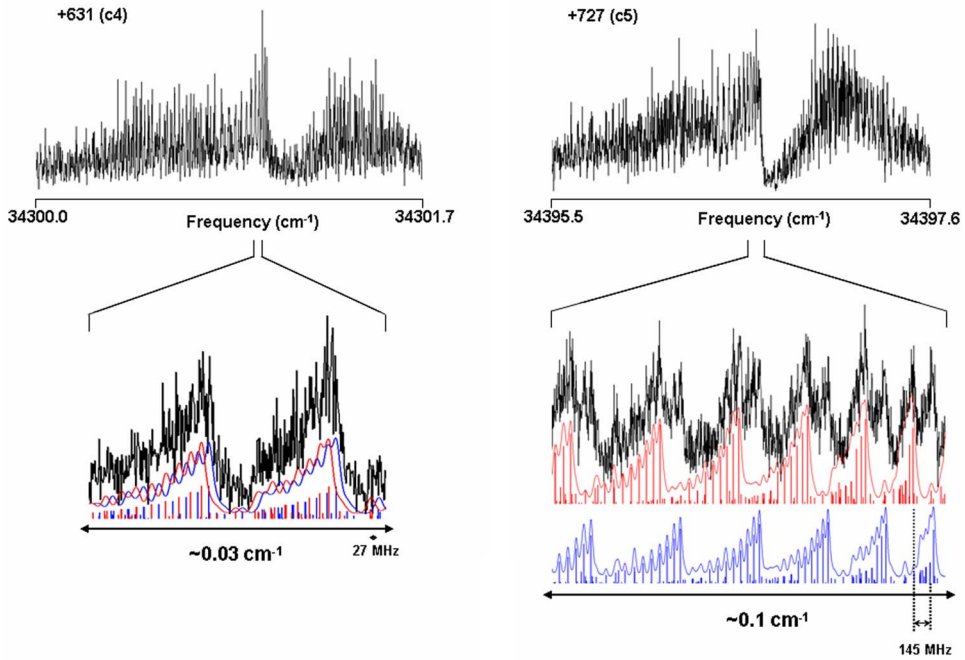

FIG. 4. Rotationally resolved fluorescence excitation spectra of the bands at +631 (**c4**) and +727 (**c5**) in the third Franck-Condon progression of DHPH in the gas phase (top panels). Similar proportions of their *Q* branches at full experimental resolution and the corresponding simulated spectra are also shown. Note that these bands require two simulated spectra to fit their corresponding experimental traces; the subband splittings are ~27 and ~145 MHz, respectively.

tions. The final fits utilized ~200 assigned rovibronic transitions and resulted in standard deviations of 2.56 and 2.97 MHz, respectively. More detailed illustrations of the quality of the fits are shown in the bottom panel of Fig. 2. Line shapes of individual rovibronic transitions were fit to Voigt profiles having Gaussian and Lorentzian components of 18 and 25 MHz, respectively. Rotational temperatures used for the fits were 5.5 and 4.5 K, respectively. Similar experiments were performed on four other members of the main progression; 0_0^0, **a1**, **a2**, and **a4**.

Several transitions in the minor **b** and **c** FC progressions were recorded and fully analyzed as well. For example, Fig. 3 shows the rotationally resolved $S_1 \leftarrow S_0$ fluorescence excitation spectra of the bands at +523 cm^{-1} (**b3**) and +714 cm^{-1} (**b5**). Each spectrum spans ~2 cm^{-1} and again exhibits 100% *a*-type character. Similar strategies were used to fit these bands; comparisons of experimental and simulated portions of these bands are also shown in Fig. 3. The standard deviations of the fits are 3.24 and 3.53 MHz, respectively. Each spectrum exhibits a Voigt profile having 18 MHz Gaussian and 30 MHz Lorentzian contributions. The rotational temperatures of the fits are 6.0 and 5.5 K, respectively. Two other **b** bands were also examined in detail, **b2** and **b4**.

We also recorded the high resolution spectra of three members of the third FC progression, the bands located at +535 cm^{-1} (**c3**), +631 cm^{-1} (**c4**) and +727 cm^{-1} (**c5**). Anticipating results similar to these for **a** and **b** bands, similar methods were used to fit the **c** progression bands. Band **c3** could be fit in this way, but bands **c4** and **c5** could not. Both of these latter bands were found to be split into two subbands with different subband splittings, ~27 MHz for the **c4** band and ~145 MHz for the **c5** band (see Fig. 4). The expanded scale sections shown in the bottom panels of Fig. 4 clearly show the remarkable differences in structure of these two bands. Rigid rotor Hamiltonians were again used to fit the observed subbands, all of which were again found to be 100% *a*-type. The standard deviations of the fits are 3.54, 3.11, and 2.56 MHz for the **c3** band and the redshifted subbands of **c4** and **c5**, respectively, and 2.08 and 3.74 MHz for the blueshifted subbands of **c4** and **c5**, respectively. Voigt line shape profiles were again observed; all five subbands have 18 MHz Gaussian and 25 MHz Lorentzian components, with rotational temperatures lying between 4–7 K. Inertial parameters of all studied members of the **a**, **b**, and **c** progressions in DHPH are reported in Table I.

IV. DISCUSSION

Every single member of each of the three vibrational progressions, that are observed in the electronic spectrum of DHPH and were examined here, exhibits a transition moment vector that is oriented parallel to the *a*-inertial axis of the molecule. Further, the ground state rotational constants of all examined bands are the same within experimental error (cf. Table I). Therefore, it is likely that all bands originate in the zero point vibrational level (ZPL) of the S_0 state and terminate in *different* vibrational levels of the *same* excited electronic state, presumably the S_1 state. In previous reports, ZZSL (Ref. 18) and SK (Ref. 19) have argued that the sec-

TABLE I. Inertial parameters derived from the fits of the high resolution spectra of all observed bands of 9,10-dihydrophenanthrene.

Parameter[a]	0_0^0	+98 (**a1**)	+196 (**a2**)	+293 (**a3**)	+390 (**a4**)	+427 (**b2**)	+487 (**a5**)	+523 (**b3**)	+535 (**c3**)	+619 (**b4**)	+631 (**c4**)		+714 (**b5**)	+727 (**c5**)	
											red	blue		red	blue
S_0															
A''(MHz)[b]	1526.8 (1)	1527.9 (1)	1526.8 (1)	1526.3 (1)	1526.8 (3)	1527.1 (1)	1528.1 (1)	1526.2 (1)	1529.1 (1)	1527.0 (1)	1529.7 (4)	1526.6 (4)	1529.0 (1)	1530.1 (1)	1528.3 (1)
B''(MHz)[b]	545.5 (1)	545.4 (1)	545.6 (1)	545.5 (1)	545.5 (1)	545.4 (1)	545.5 (1)	545.6 (1)	545.6 (1)	545.7 (1)	545.6 (1)	545.4 (1)	545.6 (1)	545.7 (1)	545.5 (1)
C''(MHz)[b]	412.5 (1)	412.5 (1)	412.5 (1)	412.6 (1)	412.6 (1)	412.5 (1)	412.6 (1)	412.5 (1)	412.5 (1)	412.5 (1)	412.5 (1)	412.6 (1)	412.5 (1)	412.4 (1)	412.5 (1)
S_1															
A'(MHz)	1491.6 (1)	1492.6 (1)	1491.4 (1)	1490.7 (1)	1491.1 (3)	1492.2 (1)	1492.2 (1)	1491.2 (1)	1492.1 (1)	1491.9 (1)	1492.6 (4)	1489.5 (4)	1493.8 (1)	1492.8 (1)	1491.1 (1)
B'(MHz)	546.2 (1)	546.0 (1)	546.1 (1)	545.9 (1)	545.8 (1)	545.9 (1)	545.6 (1)	546.0 (1)	546.2 (1)	546.0 (1)	546.1 (1)	545.9 (1)	545.8 (1)	546.0 (1)	545.9 (1)
C'(MHz)	405.8 (1)	405.9 (1)	406.0 (1)	406.1 (1)	406.2 (1)	406.0 (1)	406.3 (1)	406.1 (1)	406.3 (1)	406.2 (1)	406.3 (1)	406.4 (1)	406.3 (1)	406.4 (1)	406.4 (1)
Band origin (cm^{-1})	33669.9	33767.8	33865.4	33962.6	34059.8	34096.5	34156.7	34192.6	34205.2	34288.8	34301.1	34301.1	34384.4	34396.7	34396.7
OMC (MHz)	2.33	2.84	2.53	2.56	1.33	3.03	2.97	3.24	3.54	3.58	3.11	2.08	3.53	2.56	3.74
Temperature (K)	4.8	4.5	5.0	5.5	5.5	6.5	4.5	6.0	6.5	5.5	4.5	4.5	5.5	6.5	6.5

[a]Standard deviations shown in parentheses are uncertainties in the last significant figure.
[b]MP2/6-31G** values; $A''=1533.1$, $B''=546.5$, and $C''=414.5$ MHz.

ond and third progressions of vibronic bands originate in an S_2 state at ~240 cm^{-1} above the S_1 state, but the present results suggest that this is not the case. If a second excited state participated in the spectrum shown in Fig. 1, it would likely have differently polarized bands.

We have performed *ab initio* calculations[23] (MP2/6-31G** and CIS/6-31G) to complement our experimental observations. Theory suggests that DHPH has a dihedral angle $\varphi \sim 21.7°$ in its ground S_0 electronic state and $\varphi \sim 8.5°$ in the excited S_1 state (see Scheme 2), thereby explaining the extensive FC progression observed in its low resolution spectrum. Indeed, the molecule is predicted to have several fundamental vibrational modes lying below 300 cm^{-1} in its S_0 and S_1 states. These are listed in Table II. In what follows, we compare the results of theory and experiment in order to determine which vibrational motions are responsible for the observed FC progressions, and thereby characterize the dynamical behavior of the isolated DHPH molecule when it absorbs light.

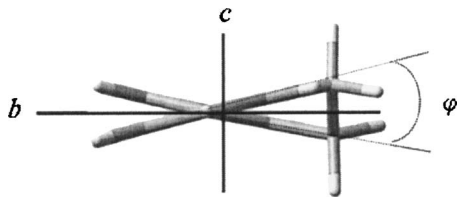

SCHEME 2. Torsional (twisting) angle φ between the two aromatic rings of DHPH.

A. The "a" progression. Symmetric out-of-plane ring twist

Of the vibrational modes shown in Table II, the most likely candidate for the first FC progression is mode 2, the symmetric ring twisting mode. Both, the symmetry of this mode (A) and its calculated frequency in the S_1 state (87.3 cm^{-1}) are consistent with what is observed experimentally (a-type bands, frequency of ~98 cm^{-1}). Other calculated modes either have the wrong symmetry (a B mode at 67.7 cm^{-1}) or lie at much higher frequency (the next A mode is predicted at 146.0 cm^{-1}).

This assignment was confirmed using the rotationally resolved spectra. Table III lists the values of the inertial defects ($\Delta I = I_c - I_a - I_b$) of each studied vibrational level in DHPH, derived from the measured rotational constants of both the ground and the excited electronic states. First, we note that all ground state values derived from fits of bands in the **a** progression are the same, within experimental error ($\Delta I = -32.4 \pm 0.2$ amu $Å^2$). This shows that all bands originate in the same vibrational level, presumably the ZPL of the S_0 state. Next, we note that the values of ΔI in the S_1 state are substantially less (in magnitude) than those of the S_0 state. This is a direct consequence of the "flattening" of the molecule, a planar molecule having a ΔI value of essentially zero.[26] Finally, we note a revealing trend; the magnitude of ΔI increases monotonically from −18.7 to −21.2 amu $Å^2$ with increasing vibrational energy, evidencing increasingly larger average displacements along some *out-of-plane* coordinate.

We have modeled this behavior in the manner shown in Fig. 5. Beginning with a geometry-optimized *ab initio* structure, DHPH was distorted from its equilibrium geometry along the symmetric ring twisting mode (φ) by 5° increments in the ground state and 1° increments in the excited state. The geometry of the molecule at each point was again energy

TABLE II. Calculated low frequency vibrational modes of 9,10-dihydrophenanthrene in its S_0 and S_1 electronic states.

Mode	Symmetry (C_2 point group)	S_0 Frequency[a] (cm^{-1})	Sketch	S_1 Frequency[a] (cm^{-1})
1. Butterfly	*B*	122.8		67.7
2. Ring twisting	*A*	140.1	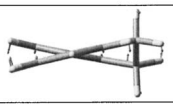	87.3
3. In-plane bending	*A*	192.9	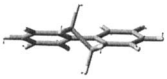	146.0
4. CH_2-CH_2 out-of-plane bending	*B*	223.4		192.8
5.In-plane stretching	*A*	275.6	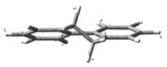	237.4
6.CH_2-CH_2 bridge deformation	*A*	333.9	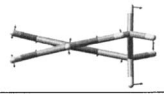	305.5

[a]Theoretical frequencies have been reduced by a factor of 0.893 (Ref. 25).

TABLE III. Inertial defects of the observed vibrational bands in the $S_1 \leftarrow S_0$ electronic spectrum of 9,10-dihydrophenanthrene. Standard deviations are ~0.05 amu $Å^2$.

Band	S_0 $\Delta I''$ (amu $Å^2$)	S_1 $\Delta I'$ (amu $Å^2$)
First Franck-Condon progression (**a** bands)		
0_0^0 (**a0**)	−32.35	−18.66
+98 (**a1**)	−32.21	−19.02
+196 (**a2**)	−32.18	−19.55
+293 (**a3**)	−32.58	−20.50
+390 (**a4**)	−32.39	−20.87
+487 (**a5**)	−32.15	−21.15
Second Franck-Condon progression (**b** bands)		
+427 (**b2**)	−32.46	−19.70
+523 (**b3**)	−32.44	−20.09
+619 (**b4**)	−31.97	−20.17
+714 (**b5**)	−31.70	−20.41
Third Franck-Condon progression (**c** bands)		
+535 (**c3**)	−31.54	−20.05
+631 (**c4**)	−31.66	−20.29
	−32.86	−21.63
+727 (**c5**)	−31.15	−20.51
	−31.91	−21.29

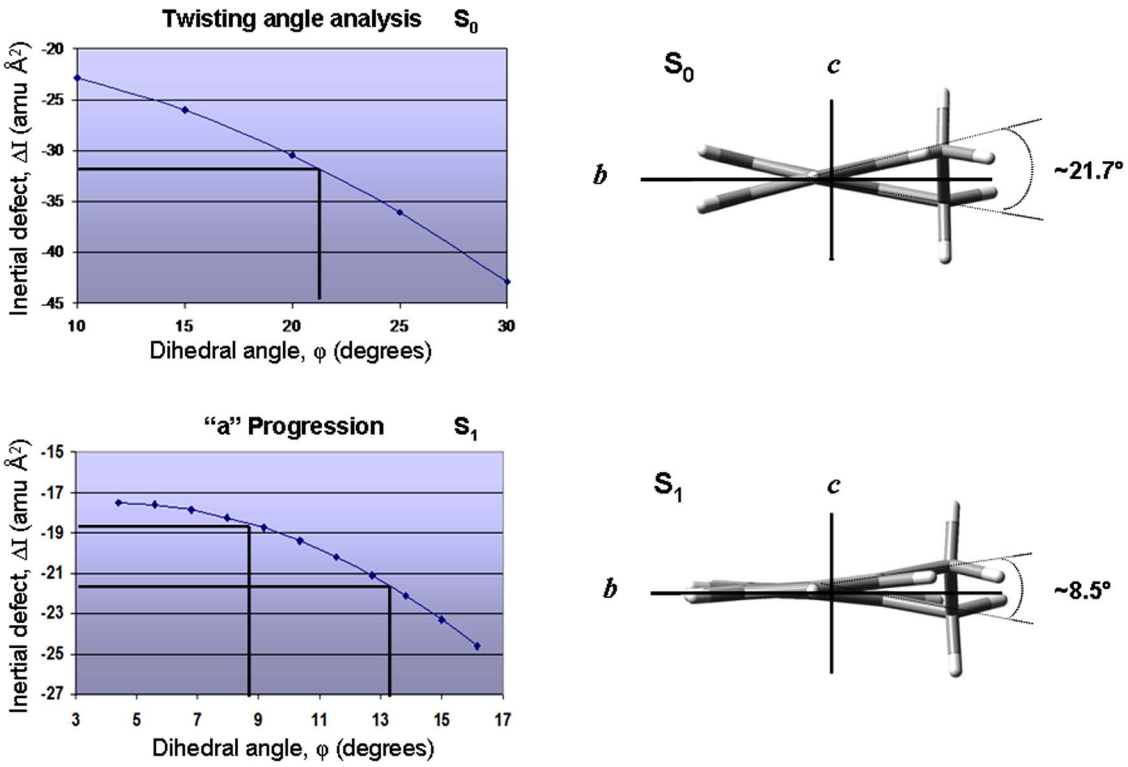

FIG. 5. Relationship between theoretical values of the inertial defect (ΔI) and the torsional coordinate (φ) for the **a** (symmetric ring twisting) mode of DHPH in its S_0 and S_1 electronic states. The range of experimental results is marked with thick lines.

optimized along all other coordinates at each step and then ΔI values were calculated. Figure 5 shows a plot of the theoretically predicted ΔI values against φ. The plot accurately reproduces the values of ΔI for a φ value in the S_0 state of $\sim 22°$ and a range of φ values in the S_1 state lying between 9 and 13°; the lower value being the one corresponding to the ZPL of the S_1 state. We thus conclude that the symmetric ring twisting mode is responsible for the major FC progression in the spectrum of DHPH. This conclusion is consistent with the earlier work of ZZSL (Ref. 18) and SK (Ref. 19) based on their careful studies of vibrationally resolved fluorescence spectra.

A crucial question that needs to be resolved is whether the potential energy surfaces (PES) along this vibrational coordinate are single or double wells in the S_0 and S_1 states. ZZSL (Ref. 18) assumed double-minimum potentials in both states, but SK (Ref. 19) argued that the potentials are single welled ones. Their calculations suggested that the suspected ring twisting mode was accompanied by a simultaneous distortion of the $-CH_2-CH_2-$ group, so that motion along this coordinate does not "carry the molecule through planarity with respect to both the rings and the aliphatic chain."[19] Since the motion is not symmetric with respect to the planar structure, the PES is single welled along this coordinate. Their arguments (for the S_1 state) were supported by the observed harmonicity of the main FC progression, and (for the S_0 state) by a fluorescence depletion experiment.

Our results confirm both of these conclusions. There is a monotonic dependence of the inertial defect ΔI on displacement along this coordinate in the S_1 state. If the potential were a double well, some "zigzag" behavior in ΔI would be expected with increasing vibrational quantum number. And no "tunneling" splittings were observed in the rotationally resolved spectra, in either state. Thus, our experimental results agree with the interpretations of SK.[19] PES's along the twisting coordinate that best represent these results are shown in Fig. 6. The S_0 minimum is located at $\varphi = 21.5°$, and the S_1 minimum is located at $\varphi = 8.5°$; the fundamental frequencies of the two potentials are 105 and 97.5 cm^{-1}, respectively. Taking harmonic oscillator wave functions for the two states, we then calculated the FC factors to estimate the frequency profile of the main vibrational progression. The best fit of the observed intensities (see Fig. 7) was accomplished by using a $\Delta\varphi$ value of $-13°$ for the dihedral angle between the two rings. This value is the same as estimated from our inertial defect analysis, confirming the "one-dimensional" model of this motion in both electronic states.

B. The "b" progression

The key observation concerning the origin of the **b** progression in the low resolution spectrum of DHPH was made by ZZSL.[18] These authors showed that a combination of three different modes appear in the dispersed fluorescence spectrum of band **b1**; at ~98, ~173, and ~265 cm^{-1}. The first mode corresponds to the ring twisting mode; the second is the in-plane bending mode; and the third is the in-plane stretching mode (cf. Table II). Thus, we assign band **b0** as a false origin (combination of the in-plane bending and in-plane stretching modes) of the $S_1 \leftarrow S_0$ transition; the calculated frequency of this "combination" band is $146.0+237.4 = 383.4$ cm^{-1} compared to an observed displacement from

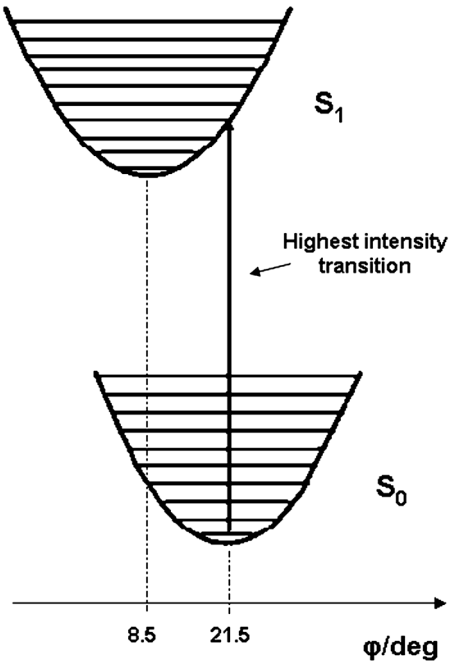

FIG. 6. Potential energy surfaces along the φ twisting coordinate that best represent the **a** progression of bands of DHPH in agreement with the experimental results.

the origin of ~234 cm^{-1}. Notably, the two contributing fundamentals are *A*-symmetry modes, explaining the *a*-type character of the band. Then, built upon this origin is a progression in the same ring twisting mode as is involved in the main progression at ~98 cm^{-1}.

Further support for this assignment is shown in the top panel of Fig. 8. Illustrated there is a comparison of measured and calculated values of the inertial defect of the S_1 DHPH vibrational levels accessed in the **b** progression. As before, $|\Delta I'|$ increases with increasing displacement along φ (cf. Table III). However, the magnitudes of these increases are less than these observed in the **a** progression. Presumably, this is because excitation of **b** bands involves displacement along an in-plane mode as well as an out-of-plane mode.

C. The "c" progression

The third FC (**c**) progression of vibrational bands exhibited in the low resolution spectrum of DHPH is even more intriguing. Again, the magnitudes of the inertial defects increase with increasing displacement along the relevant coordinate(s), as shown in Table III and the lower panel of Fig. 8. But the changes in $|\Delta I'|$ in the **c** progression are significantly larger than those on the **b** progression. Additionally, there is a nearly constant displacement of ~12.5 cm^{-1} between each pair of **b** and **c** bands. Therefore, we believe that the two progressions are "independent" in the sense that the **c** progression is built upon another false origin of different character. The most likely candidate for this origin is the "$-CH_2-CH_2-$ bridge deformation" mode, mode 6 in Table II. The calculated frequency of this mode is 305.5 cm^{-1} in the S_1 state, compared to the displacement of the **c0** band from the true origin of ~247 cm^{-1}. Additionally, all measured bands in the **c** progression are *a*-type bands; the bridge deformation mode is a totally symmetric out-of-plane mode. Then, as before, a progression of vibrations along the ring twisting mode is built upon this false origin, explaining most of the remaining vibrational activity in the spectrum.

That this interpretation of the origin of the **c** progression is correct is revealed by the remarkable finding that, whereas band **c3** (and presumably bands **c0**, **c1**, and **c2** as well) are single bands, bands **c4** and **c5** are each found to be split into two components at high resolution. The splittings of the two (equally intense) "subbands" are ~27 MHz for the **c4** band and ~145 MHz for the **c5** band. Further, as shown in Table III, the blueshifted subbands have $|\Delta I'|$ values that are larger than those of the redshifted subbands. These observations

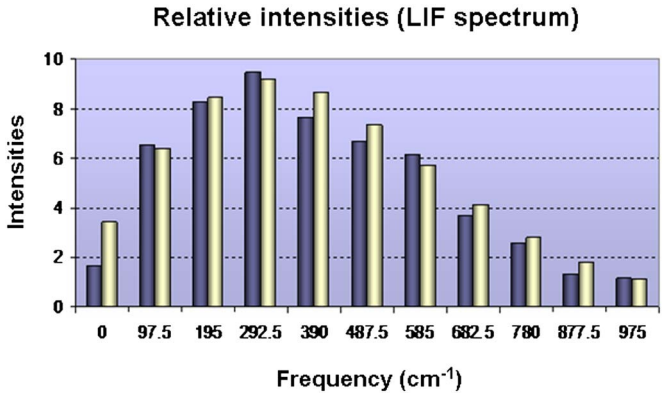

FIG. 7. Comparison of relative intensities for the **a** progression of transitions of DHPH. Dark bars correspond to the experimental results; clear bars correspond to Franck-Condon analysis.

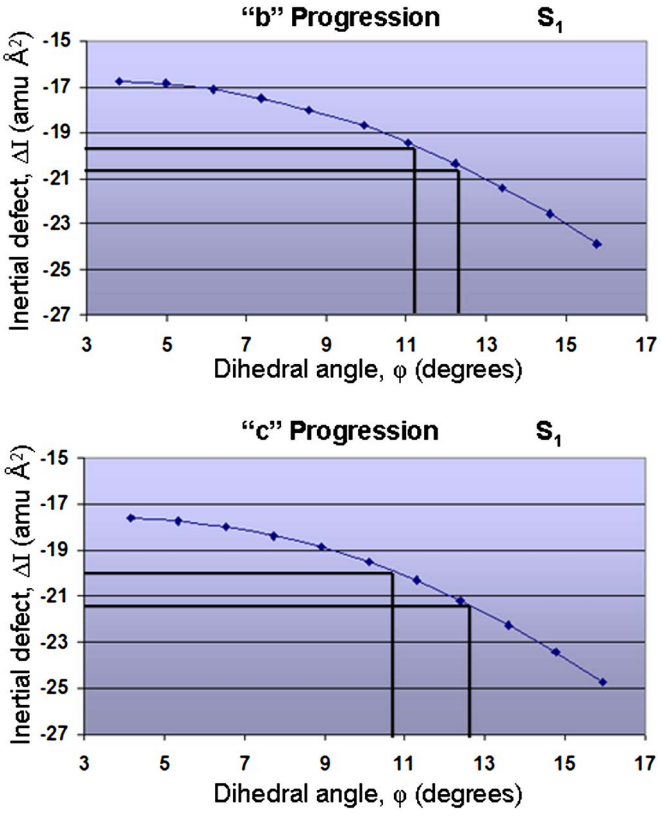

FIG. 8. Plots of the inertial defect vs. the dihedral angle for several vibrational levels in the S_1 excited state of DHPH. The top (bottom) panel shows the data for levels accessed in the **b** (**c**) progression. Points are calculated values; the solid lines indicate the range of values observed experimentally.

provide the key to understanding the nature of the tunneling motion that is responsible for the appearance of two subbands in each of these spectra, as described below.

Our model is as follows. We imagine that there is a double-well potential along Q_6, the $-CH_2-CH_2-$ bridge deformation mode, as shown in Fig. 9. Now, in the ground state, and in the zero point level of the S_1 excited state, the barrier to this motion is high. As first noted by SK,[19] "DHPH is a nonplanar molecule with a high barrier to planarity. Excitation of the ring twisting mode (mode 2) does not carry the molecule through planarity with respect to both the rings and the aliphatic chain, but does bring the phenyl rings to planarity," with respect to each other. Our results show, however, that excitation of the combined vibrational motion (one quantum in mode 6 plus one or more quanta in mode 2) does allow the molecule to pass through an "all-planar" transition state, giving rise to observable tunneling splittings with four or more quanta in the ring twisting mode. Thus, we write

$$\Psi_s = c_1\psi_1 + c_2\psi_2, \tag{1a}$$

$$\Psi_a = c_1\psi_1 - c_2\psi_2, \tag{1b}$$

where ψ_1 and ψ_2 are vibrational wave functions centered in wells 1 and 2, along the bridge deformation coordinate, and ψ_s and ψ_a are symmetric and antisymmetric combinations of these, separated by a tunneling splitting, ΔE,[27]

$$\Delta E = E_a - E_s = 2\hbar\nu \exp\left[-\frac{2\sqrt{2\mu}}{\hbar}\int_{x_1}^{0}(V(x)-E_0)^{1/2}dx\right]. \tag{2}$$

Here, ν is the vibrational frequency of mode 6, μ is the reduced mass of the molecule, $V(q_6)$ is the (assumed one-dimensional) potential energy function and E_0 is the reference energy. The potential function is centered at $x=0$, the hypothetical planar molecule. Hence, the antisymmetric state has a larger inertial defect than the symmetric one. Since the blueshifted subbands in bands **c4** and **c5** have larger $|\Delta I'|$ values, this means that the tunneling splitting (barrier height) in the S_1 excited state is larger (smaller) than in the ground S_0 state, as expected on the basis of chemical intuition.

We can calculate the barrier heights $(V-E_0)$ in the following way. Based on the calculated minimum energy geometry of the S_1 state, the two minima in the potential are estimated to lie at ±0.42 Å along the bridge deformation coordinate, this being the vertical distance of the $-CH_2-$ group above (or below) the all-planar transition state. Now, the distance to the barrier is reduced by excitation of DHPH with one quantum of the bridge deformation mode at ~254 cm^{-1}. An estimate of this distance is obtained by comparing the inertial defects of the upper state vibrational levels **a3** and **c3**, which yields $x_1=0.32$ Å. Inserting this value into Eq. (2), we find the barrier height to be ~2650 cm^{-1} if $\Delta E = 27$ MHz, and ~2150 cm^{-1} if $\Delta E = 145$ MHz. These values are believed to be accurate to ±100 cm^{-1}. Thus, the barrier to planarity along the bridge deformation coordinate is significantly (~20%) reduced by simultaneously exciting the ring

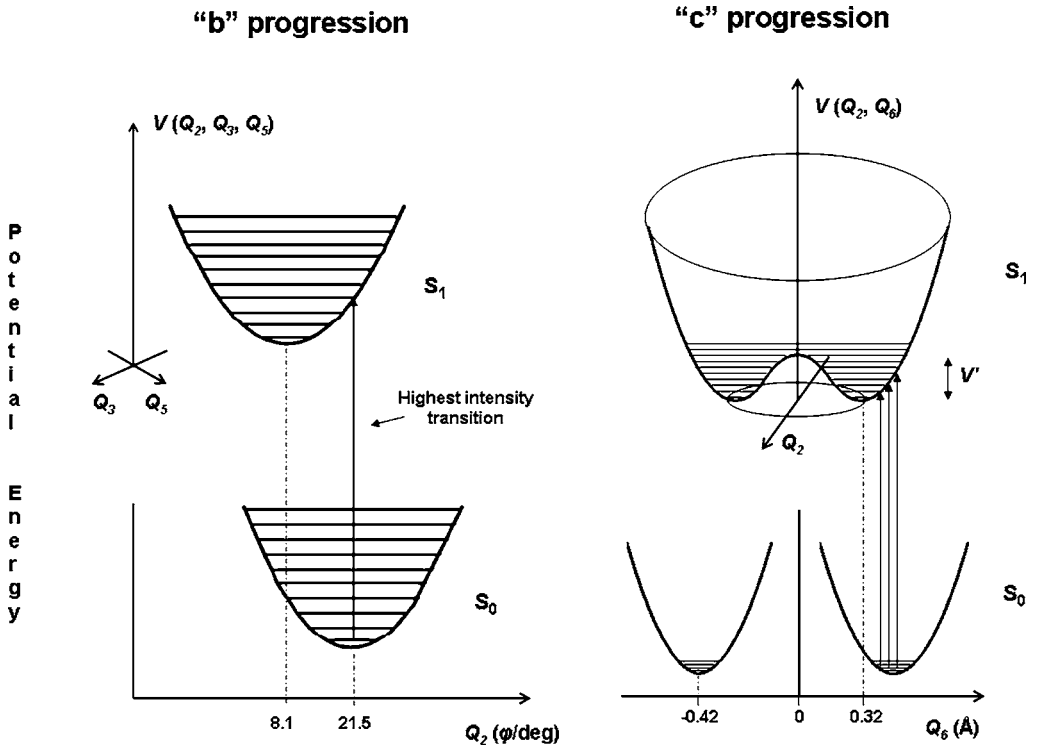

FIG. 9. Potential energy surfaces along the Q_2 (ring twisting dihedral angle/φ) for the combination of modes **b** and **c** of DHPH. The **b** progression contains two extra vibrational coordinates, Q_3 and Q_5, (inactive); whereas, the **c** progression exhibits tunneling due to the combination of the Q_2 and Q_6 ($-CH_2-CH_2-$ bridge deformation) torsional coordinates, which overcome the torsional barrier at higher energy.

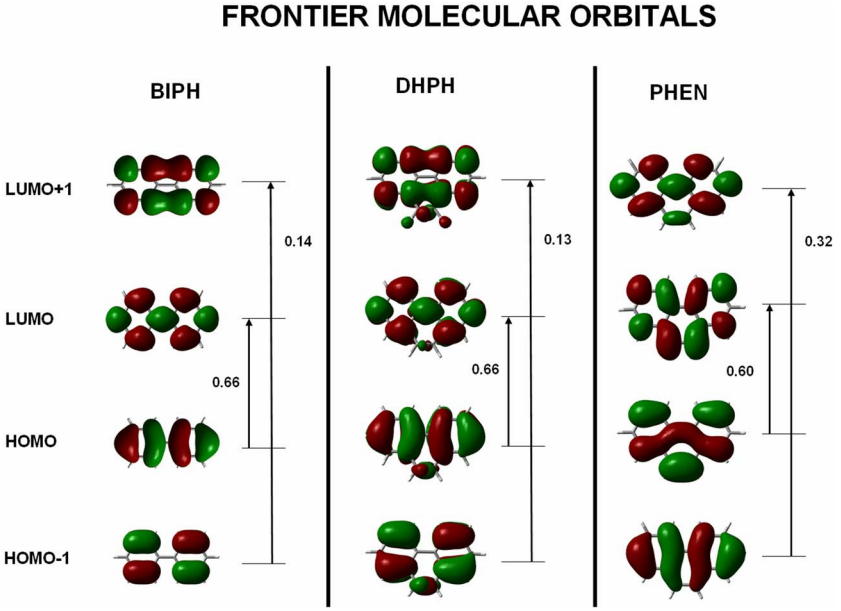

FIG. 10. CIS/6-31G frontier molecular orbitals with their corresponding transition probabilities of biphenyl (BIPH), 9,10-dihydrophenanthrene (DHPH), and phenanthrene (PHEN).

twisting coordinate, evidencing a kind of cooperative motion involving the two coordinates. A similar behavior has been observed in tropolone,[28–31] where it has been shown that the barrier to intramolecular hydrogen atom transfer from the –OH to the C═O group is substantially reduced by excitation of –C═C– stretching modes in the seven-membered ring.

Because no torsional splitting is observed in the ground state, DHPH can be regarded as belonging to the C_2 point group, having only a C_2 axis of symmetry. Then the electronic transition observed is $B \leftarrow A$. But in the excited state, when torsional splitting is observed, the C_{2v} point group is appropriate; each of the split components is a B_1, B_2 pair. Then it is useful to regard the zero point level of the S_0 state as being composed of an A_2, A_1 degenerate pair, leading to a description of the pairs of transitions in the **c** progression of DHPH as $B_2 \leftarrow A_1$ and $B_1 \leftarrow A_2$ pairs, using C_{2v} symbols for each state. It will be interesting to see if, in the future, it proves possible to resolve tunneling splittings along this coordinate in the ground state using even higher resolution methods.[32]

D. Electronic structure analysis

Though vibrational in nature, the fundamental driving force for structural change on excitation of DHPH (and tropolone) by light is electronic in nature. Figure 10 provides a comparison of the principal CIS/6-31G frontier molecular orbitals (MO's) involved in the $S_1 \leftarrow S_0$ transition of DHPH and two related molecules, biphenyl (BIPH) and phenanthrene (PHEN). The calculated MO's of DHPH and BIPH are more similar to each other, whereas those of PHEN are different. Note the reversal of the nodal patterns in PHEN, compared to DHPH and BIPH. In DHPH, the highest occupied molecular orbital→lowest unoccupied molecular orbital (HOMO-LUMO) excitation is the principal contributor to the structure of the S_1 state, bringing electron density from the periphery of the rings into the C_{12}–C_{13} bond (see Scheme 3), decreasing its bond length.

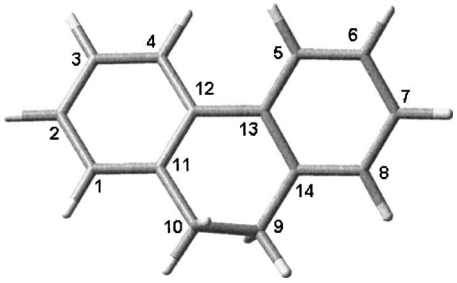

SCHEME 3. Atom numbering in DHPH molecule.

The increased conjugation between the two rings causes the molecule to become more planar in the S_1 state, as in the case of BIPH. [The relatively large change in the A rotational constant, ($\Delta A = A' - A'' = -35.2$ MHz) is a direct measure of the conjugative interaction of the two rings.] But ethane prefers to be staggered, rather than eclipsed, so DHPH is twisted in its S_1 state, rather than completely flat. Nonetheless, the competition between these two effects leads to substantial Franck-Condon activity along three different vibrational coordinates in its $S_1 \leftarrow S_0$ spectrum, as delineated here.

V. SUMMARY

Rotationally resolved $S_1 \leftarrow S_0$ fluorescence excitation spectra of three different Franck-Condon progressions of vibrational bands in the DHPH molecule reveal that the mode responsible for their appearance is the totally symmetric ring twisting mode, whose torsional coordinate of motion is the dihedral angle between the two aromatic rings (φ). The two higher frequency progressions of bands are built upon false

origins involving in-plane bending and stretching modes and a bridge deformation mode. A detailed analysis of the spectra of these bands reveals characteristics of the potential energy surface along each of these coordinates, including a coupling of two of the modes at higher energies. This coupling is a direct consequence of the second covalent link between the two aromatic rings.

ACKNOWLEDGMENTS

The authors thank Dr. John T. Yi and Dr. David R. Borst for their helpful assistance in the data analysis and Jessica Thomas for overall comments about the manuscript. This work has been supported by NSF (CHE-0615755).

[1] T. Suzuki, N. Mikami, and M. Ito, J. Phys. Chem. **90**, 6431 (1986).
[2] H. Kono, S. H. Lin, and E. W. Schlag, Chem. Phys. Lett. **145**, 280 (1988).
[3] T. G. Wright, E. Cordes, O. Dopfer, and K. Mueller-Dethlefs, J. Chem. Soc., Faraday Trans. **89**, 1609 (1993).
[4] W. E. Sinclair, H. Yu, D. Phillips, and J. M. Hollas, J. Chem. Phys. **106**, 5797 (1997).
[5] J. M. Hollas, J. Chem. Soc., Faraday Trans. **94**, 1527 (1998).
[6] W. Werncke, S. Hogiu, M. Pfeiffer, A. Lau, and A. Kummrow, J. Phys. Chem. A **104**, 4211 (2000).
[7] S. J. Baek, D. Lee, K. Choi, Y. S. Choi, and S. K. Kim, J. Mol. Struct. **611**, 203 (2002).
[8] Y. Mikami, J. Chem. Phys. **73**, 3314 (1980).
[9] K. W. Holtzclaw and D. W. Pratt, J. Chem. Phys. **84**, 4713 (1986).
[10] J. H. Frederick, E. J. Heller, J. L. Ozment, and D. W. Pratt, J. Chem. Phys. **88**, 2169 (1988).
[11] T. Chakraborty and E. C. Lim, J. Chem. Phys. **98**, 836 (1993).
[12] M. Z. Zgierski, T. Chakraborty, and E. C. Lim, J. Chem. Phys. **98**, 9340 (1993).
[13] K. Okuyama, Y. Numata, S. Odawara, and I. Suzuka, J. Chem. Phys. **109**, 7185 (1998).
[14] J. Laane, J. Phys. Chem. **104A**, 7715 (2000).
[15] M. Baba, A. Doi, Y. Tatamitani, S. Kasahara, and H. Kato, J. Phys. Chem. A **108**, 1388 (2004).
[16] See for example, H. Petek, K. Yoshihara, Y. Fujiwara, Z. Lin, J. H. Penn, and J. H. Frederick, J. Phys. Chem. **94**, 7539 (1990).
[17] T. Chakraborty and M. Chowdhury, Chem. Phys. Lett. **177**, 223 (1990).
[18] M. Z. Zgierski, F. Zerbetto, Y. Shin, and E. C. Lim, J. Chem. Phys. **96**, 7229 (1992).
[19] J. M. Smith and J. L. Knee, J. Chem. Phys. **99**, 38 (1993).
[20] W. A. Majewski, J. F. Pfanstiel, D. F. Plusquellic, and D. W. Pratt, *Laser Techniques in Chemistry*, edited by T. R. Rizzo and A. B. Myers (Wiley, New York, 1995), p. 101.
[21] N. Ohta and H. Baba, Mol. Phys. **59**, 921 (1986).
[22] Y. Takei, T. Yamaguchi, Y. Osamura, K. Fuke, and K. Kaya, J. Phys. Chem. **92**, 577 (1988).
[23] M. J. Frisch, G. W. Trucks, H. B. Schlegel *et al.*, GAUSSIAN 98, Revision A.9, Gaussian, Inc., Pittsburgh, PA, 1998.
[24] D. F. Plusquellic, JB95, spectral fitting program, NIST, http://physics.nist.gov/jb95
[25] J. B. Foresman and Æ. Frisch, *Exploring Chemistry with Electronic Structure Methods*, 2nd ed. (Gaussian Inc., Pittsburgh, PA, 1996), p. 64.
[26] T. Oka and Y. Morino, J. Mol. Spectrosc. **6**, 472 (1961).
[27] R. P. Bell, *The Tunnel Effect in Chemistry*, (Chapman and Hall, New York, 1980), p. 43; for numerical methods of analysis, see J. R. Letelier and A. Toro-Labbé, J. Math. Chem. **39**, 485 (2006).
[28] A. C. P. Alves and J. M. Hollas, Mol. Phys. **23**, 927 (1972).
[29] A. C. P. Alves and J. M. Hollas, Mol. Phys. **25**, 1305 (1973).
[30] R. K. Frost, F. Hagemeister, D. Scheleppenbach, G. Laurence, and T. S. Zwier, J. Phys. Chem. **100**, 16835 (1996).
[31] J. J. Paz, M. Moreno, and J. M. Lluch, J. Chem. Phys. **108**, 8114 (1998).
[32] Referee comments.